

Overtured-wave migration by two-way extrapolation

Zhiming Li, Jon F. Claerbout and Richard A. Ottolini

Abstract

Overtured waves are the reflections from the undersides of steeply dipping reflectors. Conventional depth migration usually treats them as evanescent waves and ignores them when downward continuing the wave field. To migrate the overtured waves, the reverse time migration method based on the two-way non-reflecting wave equation was suggested by Baysal, Kosloff and Sherwood (1984). As an alternative approach to handle the same problem, a two-way extrapolation method to migrate the normal and the overtured reflections separately was recently proposed by Claerbout (1984).

The principle of Claerbout's two-way extrapolation method and some practical computation examples are discussed in this paper.

Introduction

Migration by depth extrapolation is usually done by downward continuing the wave field observed on the surface to various depths of exploration interests. Using the exploding reflector concept (Claerbout, 1982), zero-offset time section can be regarded as seismogram recording the waves which are generated from the reflectors and propagate with half rock velocities. The dispersion equation used in the phase-shift migration has the restriction that waves generated from exploding reflectors must travel only upwards at any depth. The other energy which goes beyond the limit is said to be evanescent, and is ignored or set to zero.

By separating the wave field into downward-going and upward-coming components, the path of an overtured wave can be divided into two subpaths: one goes downward until it

hits a turning point, the other comes upward after the turning point. In applying the downward extrapolation, the upward component of wave field is migrated down to the reflectors or the turning points. After the downward extrapolation, the upward extrapolation of the evanescent energy saved in the first pass of continuation will migrate the downward component to the reflectors' positions. Thus, one image of the normal reflection and another of the overturned reflection are made. Therefore, overturned reflections can also be migrated to give us more information about the subsurface structure.

Simply normalizing and summing the two images can enhance the resolution of steeply dipping reflectors; this enhancement can be useful in determining some geological features such as faults or salt domes. Further more, the precision of velocity analysis and reflectivity estimation may be done more precisely by studying both the geometrical and the amplitude relationships between these two images.

Separating ray path

A zero offset section can be analyzed by use of the exploding reflector concept, which is that rays are generated at exploding reflectors and received at the earth surface. Each ray's path can consist of two subpaths, one going down, one coming up. A normal reflection has only upward path, but an overturned reflection has both downward and upward paths, as shown in Figure 1.

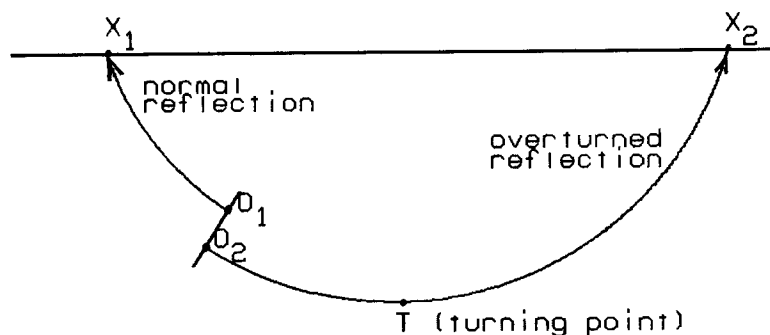


FIG. 1. Normal reflection O_1X_1 has only upward raypath. Overturned reflection O_2X_2 has downward path O_2T and upward path TX_2 . O_1 and O_2 are the exploding reflectors.

Two-way extrapolation

The depth extrapolation of the wave field $P(\omega, k_x, z)$ from depth z to depth $z + \Delta z$ is based on the following equations:

$$P(\omega, k_x, z + \Delta z) = P(\omega, k_x, z) e^{i k_z \Delta z}, \quad (1)$$

$$k_z(\omega, k_x) = -\frac{\omega}{v(z)} \sqrt{1 - \frac{v^2(z) k_x^2}{\omega^2}}, \quad (2)$$

where $P(\omega, k_x, z)$ denotes the 2-D Fourier transform of data $P(t, x, z)$, and $v(z)$ is one half of the rock's velocity.

The dispersion relation (equation (2)) has the constraint that energy must travel upward. The downward energy that satisfies $|v k_x / \omega| > 1$ is called evanescent energy because the square root is imaginary. The conventional way of processing of evanescent energy is simply not to incorporate it into the computation of the field at each depth. The extrapolation operator thus applies only to the region $|v k_x / \omega| \leq 1$, as depicted on Figure 2.

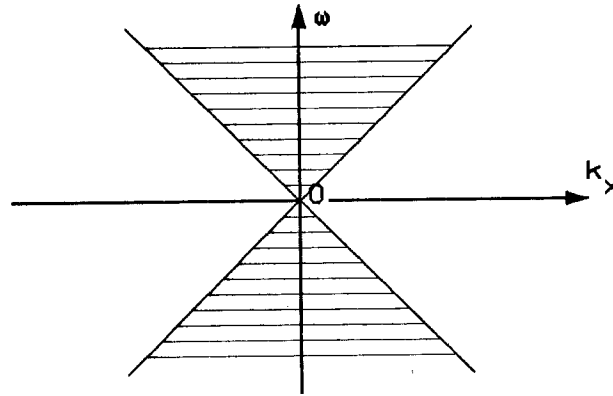


FIG. 2. The extrapolation operator $\exp(-i \omega \Delta z \sqrt{1 - v^2(z) k_x^2 / \omega^2} / v(z))$ applies only to the shaded region $|v k_x / \omega| \leq 1$.

In a medium with linearly increasing velocity, this shaded region narrows as downward continuation goes deeper.

Equations (1) and (2) relate the wave field $P(\omega, k_x, z + \Delta z)$ at depth $z + \Delta z$ and the field $P(\omega, k_x, z)$ at depth z in transform domain, providing that the forward Fourier kernel is $\exp(i \omega t - i k_x x)$. When the wave field has been downward continued through different depths to the maximum depth, the normal reflection (Figure 1, $O_1 X_1$) is migrated to the exploding reflection point, O_1 , giving the image of the top of the reflector. However, the

overtaken reflection, O_2X_2 , is migrated only to the turning point, T , because the downward extrapolation using equations (1) and (2) migrates only the upcoming waves. The overtaken reflection field stops being migrated when the energy of this field lies outside the shaded region in Figure 1 and becomes evanescent. This partially migrated energy is saved at its turning point for the further processing.

In order to continue migrating the energy overtaken at the turning point (Figure 1, T) to the exploding reflector (Figure 1, O_2), an upward extrapolation is needed. Because such a second pass of upward migration is still used to extrapolate the wave field toward the exploding reflector as the first pass of downward continuation, equations (1) and (2) are still valid for the upward extrapolation. The shaded region in Figure 2 will widen as the operator moves higher. The partially migrated overtaken energy saved in the first pass migration is thus reintroduced and extrapolated upwards to generate an image of the underside of the steeply dipping reflector. Finally both images of the upside and the underside of the reflectors are constructed.

Two examples

In order to test this method we generate two synthetic examples. The first consists of normal and overtaken reflections from a single reflector. The second example is of a geologically more realistic model of a reverse fault.

In a linear velocity medium (i.e., velocity varies linearly with depth), the receiving position and the arrival time of a normal reflection can be expressed (Slotnick, 1959) as:

$$x_n = x_e - \frac{1}{ap} \left[\sqrt{1 - p^2 v_0^2} - \sqrt{1 - p^2 v^2(z)} \right], \quad (3)$$

$$t_n = \frac{2}{a} \ln \left\{ \frac{v(z) \left[1 + \sqrt{1 - p^2 v_0^2} \right]}{v_0 \left[1 + \sqrt{1 - p^2 v^2(z)} \right]} \right\}, \quad (4)$$

while equations (5) and (6) define the receiving position and the arrival time for an overtaken reflection:

$$x_o = x_e + \frac{1}{ap} \left[\sqrt{1 - p^2 v_0^2} + \sqrt{1 - p^2 v^2(z)} \right], \quad (5)$$

$$t_o = \frac{2}{a} \ln \left\{ \frac{\left[1 + \sqrt{1 - p^2 v_0^2} \right] \left[1 + \sqrt{1 - p^2 v^2(z)} \right]}{p^2 v_0 v(z)} \right\}, \quad (6)$$

where (x_e, z) is the position of the reflector point, $p = \sin\theta / v(z)$ the ray parameter at (x_e, z) , θ the dip of the reflector at (x_e, z) . As shown on Figure 3, the velocity function is $v(z) = v_0 + az$.

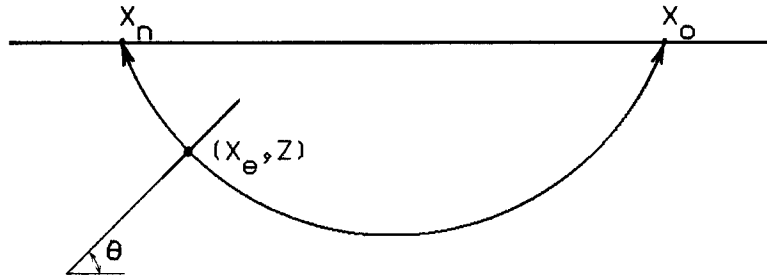


FIG. 3. A reflector at (x_e, z) generating the normal reflection received at x_n and the over-turned reflection received at x_o . The velocity function is $v(z) = v_0 + az$.

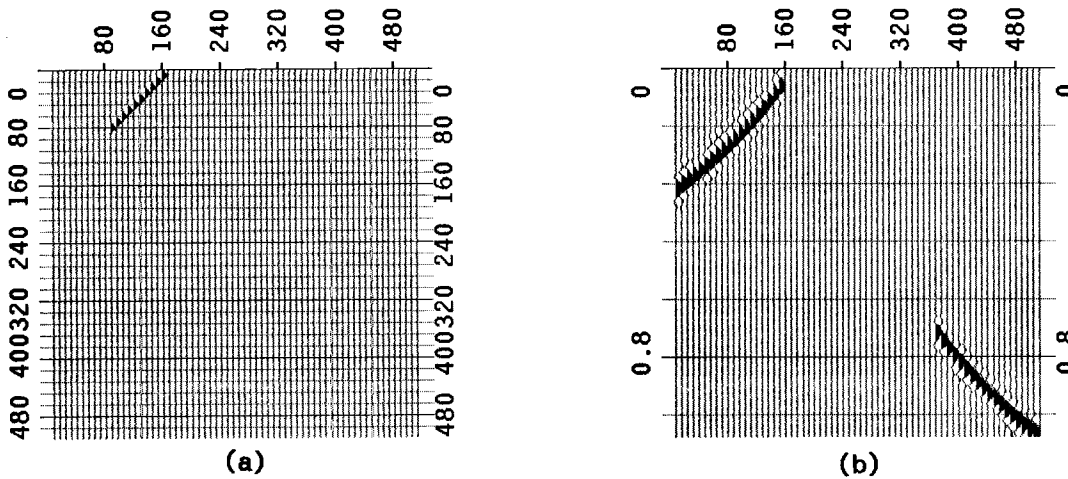


FIG. 4. (a) A model of a 45° dipping reflector. The velocity function is $v(z) = 500 + 5z$. (b) A zero-offset time section of the model depicted in Figure 4 (a). It is calculated by using equations (3)-(6). Normal reflection is on the upper left corner, and overturned reflection on lower left corner.

Figures 4 and 5 show the separate processings of the normal reflection and the overturned reflection that are generated from a segment of 45° dipping reflector. As expected, the downward extrapolation handles only the normal reflections, and the upward extrapolation deals only with the raypaths between reflectors and turning points. Using both extrapolations migrates completely the overturned reflections.

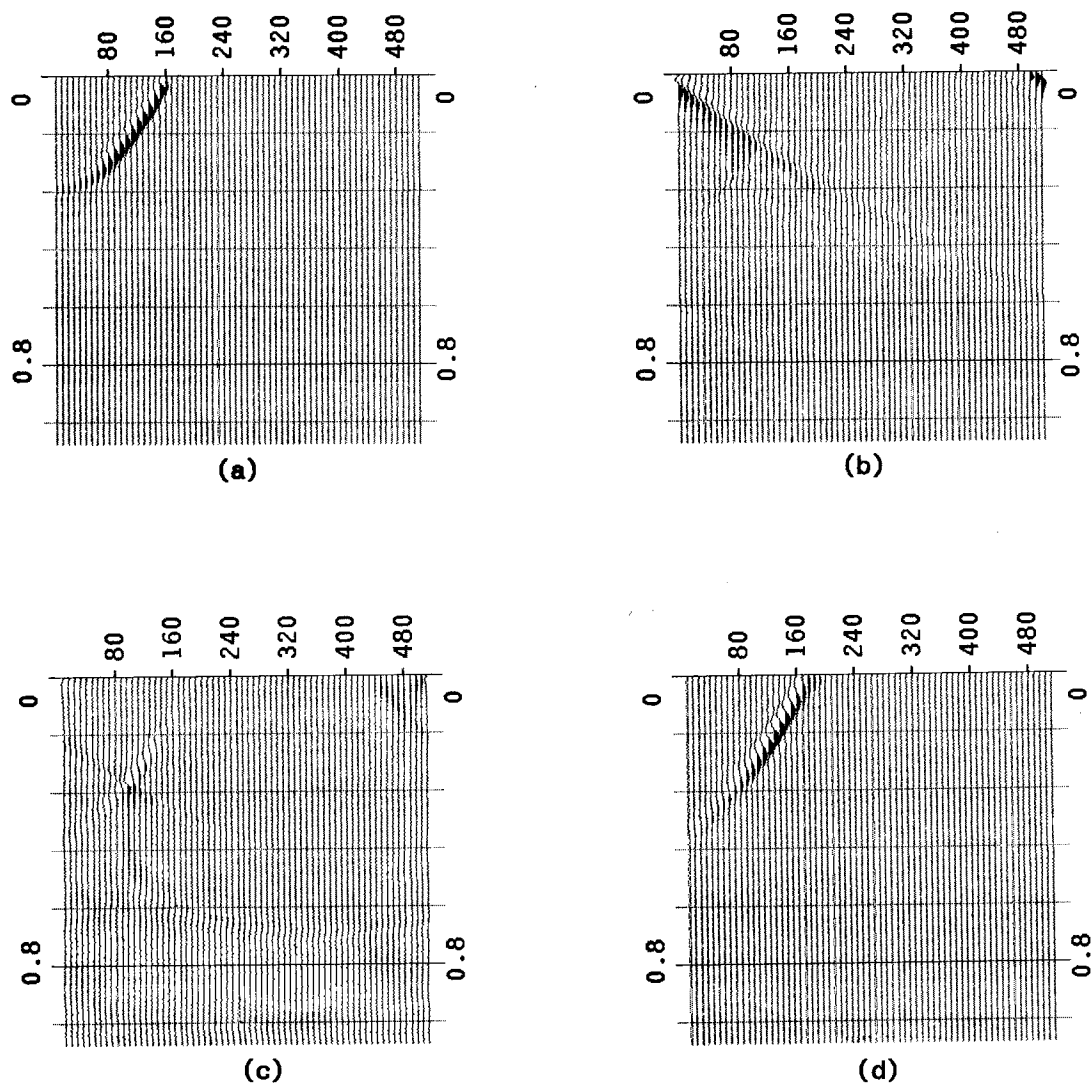


FIG. 5. Results of migrating the data shown on Figure 4. (a) Migrated time section of the normal reflection by the downward extrapolation. (b) Migrated time sections of normal reflection by the two-way extrapolation. (c) Migrated time sections of the overturned reflection by the downward extrapolation. (d) Migrated time sections of the overturned reflection by the two-way extrapolation.

A geologically more realistic model was also constructed, which can be analogous to a reverse fault. To simplify the calculation, the effects of magnitudes of reflection coefficients, transmission, attenuation and multiple reflections are not incorporated into the modeling. Figure 6 shows the model and its synthetic seismogram. The normal reflections from the tops of reflectors are present in Figure 6 (b) along with an overturned reflection from the underside of the overthrust fault plane.

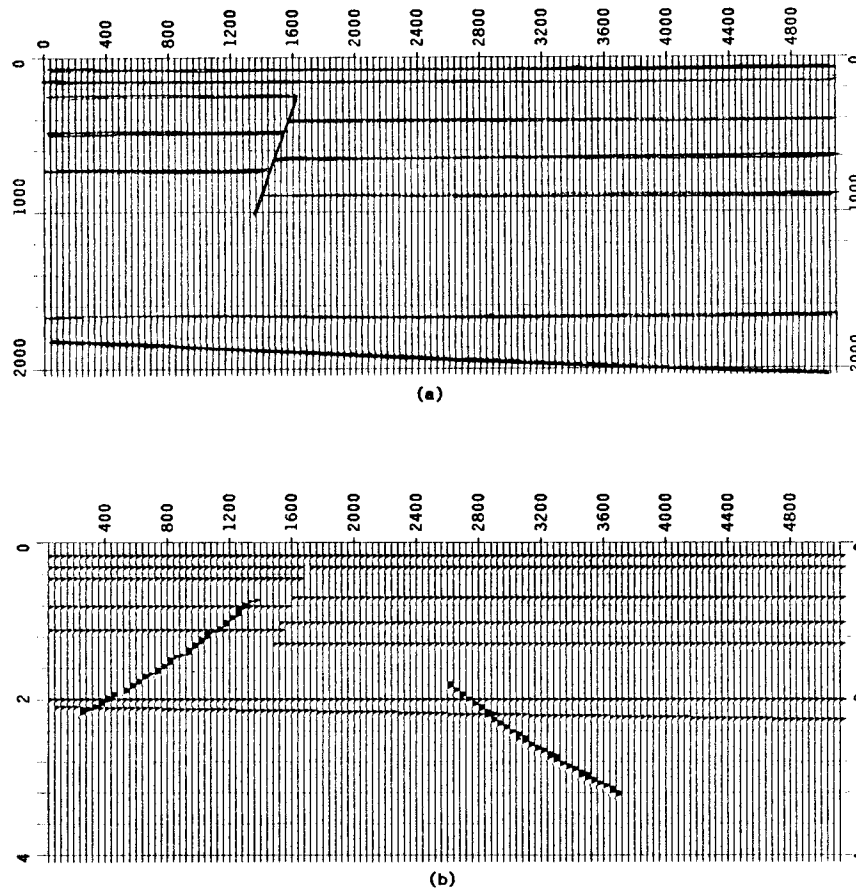


FIG. 6. (a) A model of a 70° reverse fault, with the velocity function $v(z)=1000.+z$ (meters/sec.). (b) Synthetic seismogram of the model. The normal reflection of the fault plane is shown on the upper left. Overturned reflection of the fault plane is on the lower right.

The migrated time sections of upward extrapolation and downward extrapolation are shown on Figure 7 (a) and (b), respectively. The two different images of the overthrust fault plane fit exactly at the same proper place. Normalizing and summing these two results together gives a stronger indication of the fault plane than the conventional downward extrapolation result shown in Figure 7 (a). The summed depth section is shown on Figure 8.

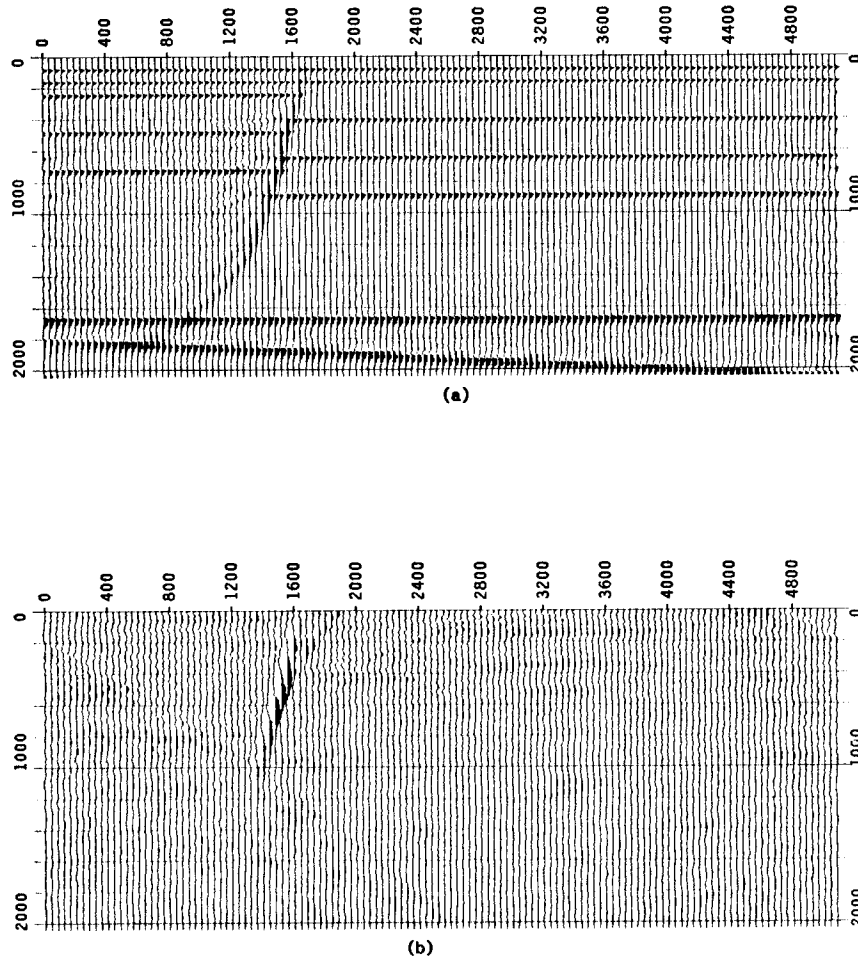


FIG. 7. (a) Migrated depth section by first pass of downward extrapolation. (b) Migrated depth section by two-way extrapolation.

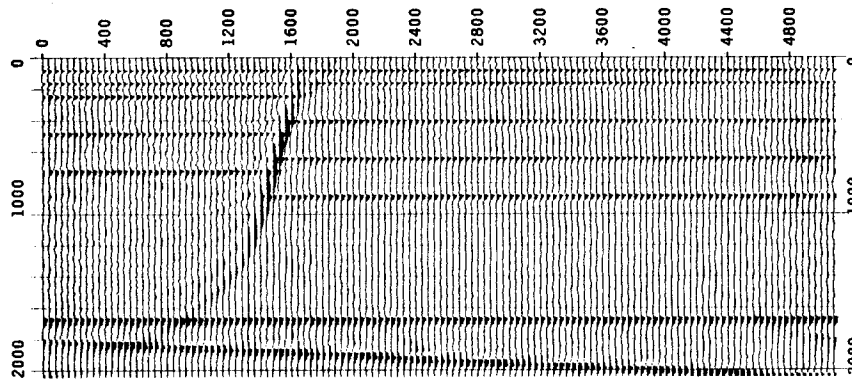


FIG. 8. Final migrated depth section by combining (a) and (b) in Figure 6. The fault plane image has been significantly enhanced.

Conclusion

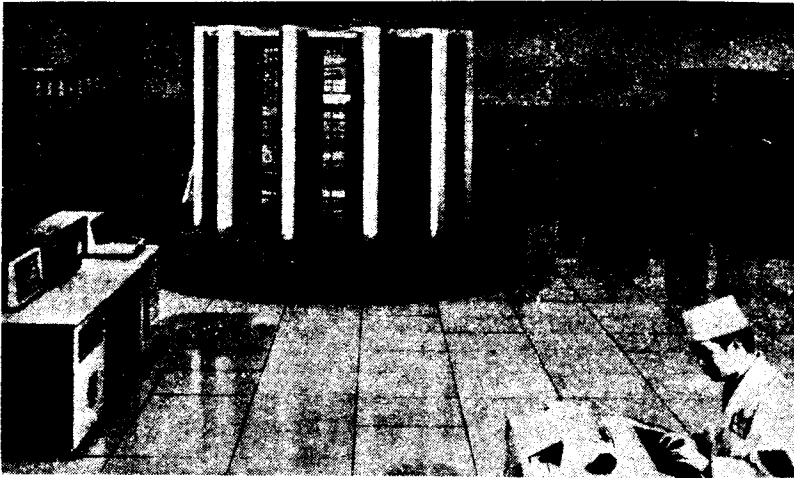
Claerbout's two-way extrapolation can migrate both the normal reflection and the overturned reflection. It offers the means to image both sides of steeply dipping reflectors, and enhances the resolution of such reflectors. The velocity distribution above a fault plane may be estimated by comparing the relative migrated positions of normal and overturned reflections. Because two reflections from both sides of the reflectors can be taken into consideration simultaneously, the two-way extrapolation may also increase the accuracy of estimating the reflection coefficients of a steeply dipping reflector,

ACKNOWLEDGMENTS

The authors thank John W.C. Sherwood for sending his co-authored paper " A Two-way Non-reflecting Equation ", which gives another approach of dealing with the overturned reflection problem.

REFERENCES

- Baysal, E., Kosloff, D.D., and Sherwood, J.W.C., 1984, A two-way nonreflecting wave equation: *Geophysics*, v.49, p.132-141.
 Claerbout, J.F., 1982, *Imaging the earth's interior*: California, Stanford University.
 Ottolini, R.A., 1982, migration of reflection seismic data in angle-midpoint coordinates: *SEP-33*, p.64-68.
 Slotnick, M.M., 1959, *Lessons in seismic computing*: Wisconsin, George Banta Company.



The main machine of the "Galaxy" super-computer at work.

over the past two decades, as shown by the successful launch of a series of man-made earth satellites and space rockets. However, this is the first breakthrough in super-computer technology.

'Galaxy' Super-Computer

China has successfully produced its first super-computer, capable of performing more than 100 million operations per second. Its smooth operation has already been certified by the state.

The "Galaxy" super-computer was developed by the research staff of the University of Defence Science and Technology after six years of continuous effort. Some 20 other research institutes and production departments across the country also contributed to the effort.

Beginning in May 1983, the State Council organized 95 computer experts and technicians from 29 departments throughout the country to begin examination of the finished computer. The super-computer had an uninterrupted trial run of more than 13,000 hours. The results proved the computer system to be reliable, correct, advanced and up to the national standard.

There are now only a few countries in the world able to produce super-computers. The success of China's "Galaxy" super-computer will narrow the technological gap between China and the advanced countries, and marks a new phase in Chinese computer sciences.

China began to produce its own computers in the early 1960s. Rapid progress has been made